19th Brazilian Congress of Thermal Sciences and Engineering
November 6th–10th, 2022, Bento Gonçalves - RS - Brazil

ENC-2022-0431
Study of the Impact of MicroCT Image Resizing on Numerically Estimated Porosity and Permeability Data

Ingrid B. Carneiro
Celso P. Fernandes
Dept. de Engenharia Mecânica, Universidade Federal de Santa Catarina (UFSC). Campus Universitário Reitor João David Ferreira Lina, Trindade, Florianópolis, 88040-900, Santa Catarina, Brasil.
ingrid.bertin@posgrad.ufsc.br, celso@lmpt.ufsc.br

Fabio L. Bagni
Petrobras, E&P, EXP. Av. Henrique Valadares, 28 - 2º andar - Centro, 20231-030 - Rio de Janeiro, Barzil.
fabiobagni@petrobras.com.br

Francisco H. R. Bezerra
Dept. de Geologia, Universidade Federal do Rio Grande do Norte (UFRN). Campus Universitário, Rua das Engenharias, s/n, Lagoa Nova, Natal, 59078-970, Rio Grande do Norte, Brasil
bezerrafh@geologia.ufrn.br

Abstract. *Estimating petrophysical properties from high quality core-plug images can become computationally expensive, taking days. To address this problem, resample algorithms such as the Lanczos algorithm can be applied to the grayscale image or binary image, decreasing the quality and consequently reducing the computational cost of the simulations. In this work, we propose a study to assess the impact of resizing using the Lanczos algorithm, increasing from 1.1 to 2 times the image resolution size, on the estimated porosity and permeability values. Stokes equations are used to model the single-phase flow inside the porous space. These equations are discretized using the Finite Volume Method implemented in the OpenFOAM software. Simulation results show that the resample performed on the grayscale images showed porosity closer to the original values and the permeability values in the same order of magnitude. Furthermore, after analyzing the results, we verify that the computational cost associated to the simpleFoam solver used to solve the flow problem was much lower. To ensure the reliability of the results, they were compared with those obtained experimentally.*

Keywords: *3D image processing, pore-scale simulation, brazilian outcrop*

1. INTRODUCTION

Petrophysical properties like porosity and permeability are fundamental in a reservoir area because they're inputs for reservoir characterization. Moreover, they impact a variety of different rock properties like rock density, thermal conductivity as well as geomechanical parameters (Bohnsack *et al.*, 2020; Weinert *et al.*, 2021). Core analysis laboratories have for years provided physical rock properties through experiments performed on core plugs. However, to estimate petrophysical rock properties experimentally takes a lot of time (Al-Marzouqi, 2018).

Currently, with the advances in the micro computed tomography (microCT) area, it was possible not only a greater visualization of the internal structure of the rock but also to numerically estimate rock properties. This combination of microtomographic imaging and simulation is known as Digital Rock Physics (DRP). DRP is faster than the experimental analysis, but to ensure a good solution, several authors recommend, in the case of direct simulation methods, that the cell size is smaller or equal to that of a voxel size (Arns *et al.*, 2005; Mostaghimi *et al.*, 2013; Soulaine *et al.*, 2016) having a high computational cost and requiring powerful computers.

To address this problem, resample algorithms such as the Lanczos algorithm can be applied to the grayscale image, decreasing the quality and consequently reducing the computational cost of the simulations. Several authors have studied the impact that resizing has on properties such as porosity and permeability (Peng *et al.*, 2012; Al-Ansi *et al.*, 2013; Alyafei *et al.*, 2015; Latief *et al.*, 2017).

Peng *et al.* (2012) studied Berea sandstone with two resolutions ($0.35\ \mu m$ and $12.7\ \mu\ m$) to evaluate the resolution

effect. They found that both low- and high-resolution generated better results in surface area, especially for smaller pores. However, low-resolution images overestimated the pore size and pore connectivity.

Al-Ansi *et al.* (2013) studied the impact of the resolution of the images of two sandstones on the porosity and permeability results obtained by pore networks. They demonstrated an low variation of porosity to image resolution, while permeability vary significantly.

Alyafei *et al.* (2015) studied the impact of the resolution of the images of four rocks samples, Berea and Doddington sandstones and Estaillades and Ketton limestones, on the porosity and permeability results. In this work, the Lanczos algorithm was used to perform the resizing from the segmented images. They concluded that the image porosity is relatively insensitive to resolution for both sandstone rocks, but, for the limestones, the porosity increases as a function of voxel size.

Latief *et al.* (2017) studied the effect of the image resolution obtained by means of hardware-based (acquisition using increased pixel binning of the camera) and software-based approach (during the reconstruction process). They concluded that simulating fluid flow through the pore space using the Lattice Boltzmann method to calculate the permeability has a strong dependency on the image resolution.

In this study, we evaluated the impact that the resizing of the images of two subsamples of core plugs of carbonate rocks has on the estimates of porosity and permeability values. In resizing was used the Lanczos algorithm. This resizing is done after the images cropping stage, i.e., on the grayscale images before any filter passes, contrary to the one employed by (Alyafei *et al.*, 2015) that did the resizing after the binarization.

2. MATERIALS AND METHODS

This section describes all the steps used in this work to obtain the porosity and permeability results from microCT images. First, the microCT grayscale image is pre-processed and segmented aiming to determine the void space that is the phase of interest used to build the computational grid. Then, the mathematical model and the setup for flow simulations is defined.

2.1 Images acquisition and Pre-processing

The two rock subsamples we used in this study are subsamples from samples of carbonate rocks of the Jandaíra Formation, that was subjected the karstification process, gathered from Brazilian state of Rio Grande do Norte. They are imaged using Versa XRM-500 (Zeiss/XRadia) X-Ray Microtomography that provides the three-dimensional (3D) 16-bit grayscale color images, whose volumes can be seen from Fig. 1 below. The volumes and voxel sizes can be seen in Tab. 1.

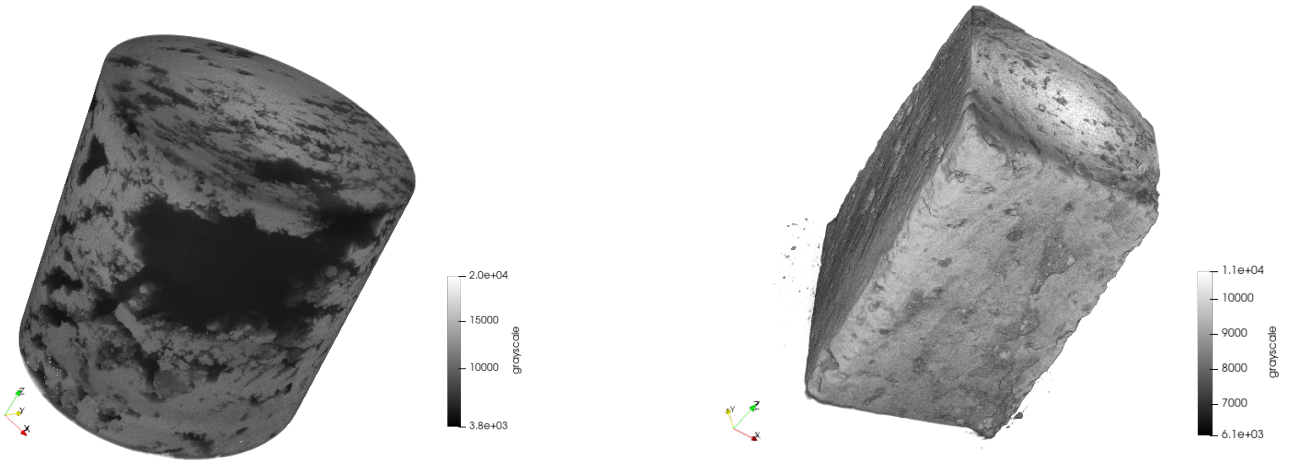

(a) Sample 1 (b) Sample 2

Figure 1: 3D volumes of the microCT images in grayscale from the samples (a), (b).

Table 1: MicroCT image information of voxel and volume sizes.

MicroCT image	Sample 1	Sample 2
Voxel size (μm)	5.57	4.48
volume size (voxel3)	992x1012x996	988x1012x996

First, cropping is done to remove all slices with cone-beam artifacts, derived from the fact that microCT scanner acquires from circular trajetory only and does not provide sufficient sampling for reconstruction algorithm (Semmler and

Schwaiger, 2008; Han and Baek, 2019). The final size of the images after the cuts are described in Tab. 2.

Table 2: MicroCT image information of voxel and subvolume sizes.

MicroCT image	Sample 1	Sample 2
Voxel size (μm)	5.57	4.48
Subvolume size (voxel3)	506x529x950	988x1012x960

After cropping, these images are resampled multiplying the image resolution by factors 1.1, 1.2, 1.3,$\cdots$, 2 using the Lanczos resampling algorithm, present in the commercial software Avizo® 8.1 (FEI, 2014).

Lanczos is an interpolation method that is defined by a kernel function given by the product of the normalized $sinc$ function and the Lanczos window (Distante and Distante, 2020).

After resample, these images are pre-processed applying a Non-Local Means filter (Buades *et al.*, 2005) to denoise and an Unsharp Mask (Sheppard *et al.*, 2004) to emphasize texture and details. Then, they are segmented in two phases, void space and rock matrix using threshold grayscale values as shown in Fig. 2. These thresholds were defined from the identification in the images of voxels with darker colors that represent the void space while brighter grayscale values correspond to the rock grains.

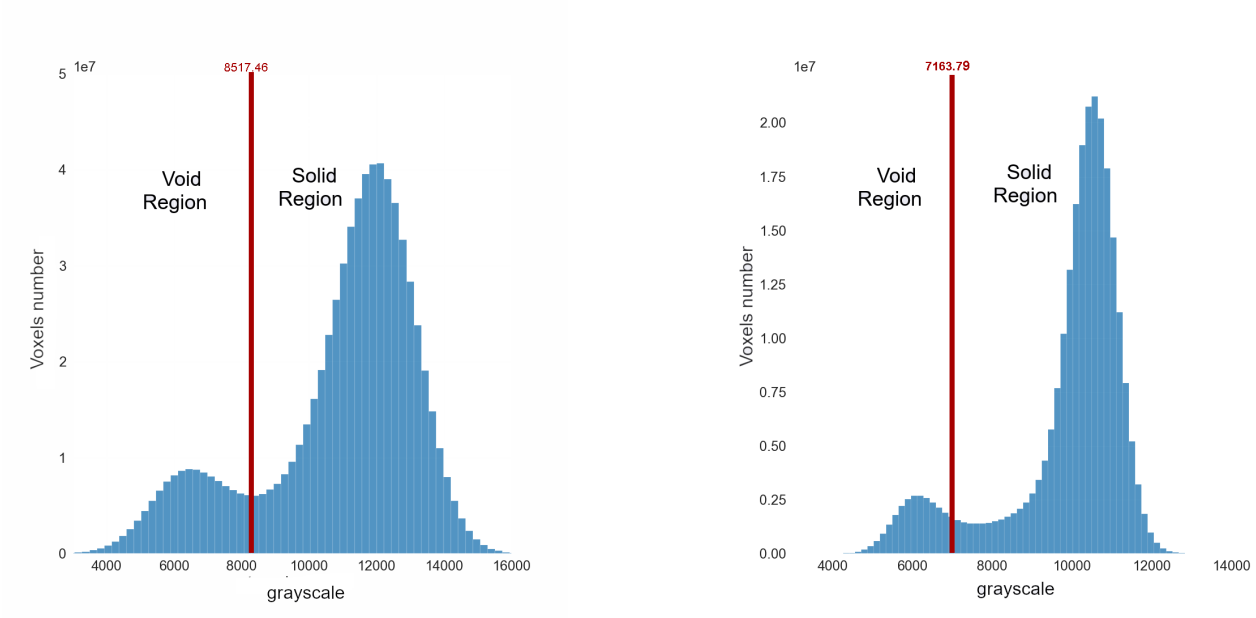

(a) Sample 1 (b) Sample 2

Figure 2: Grayscale histogram from the samples (a), (b).

The changes of the pore space after resample and segmentation of the images, with initial and final resolutions, is shown in the Fig. 3-4. Observing the images we can assume that the pore space variation is small.

2.2 Mathematical model

Considering water as a percolating fluid, incompressible flow and stationary state, single-phase flow in porous media can be described by Stokes equations given by:

$$\nabla \cdot \mathbf{v_f} = 0, \tag{1}$$

$$-\frac{1}{\rho}\nabla p + \nu \Delta \mathbf{v_f} = \mathbf{0}. \tag{2}$$

where p is the pressure, ν is the kinematic viscosity, $\mathbf{v_f} = (v_{fx}, v_{fy}, v_{fz})$ is the fluid velocity and ρ is the fluid density. Once that the values of pressure and velocity are obtained, the permeability component in z-direction can be obtained from:

$$k_{zz} = \mu \left(\frac{L_z}{\Delta p}\right)\left(\frac{1}{V}\int_V u_z dV\right), \tag{3}$$

where Δp is the pressure drop, L_z is the sample length in the z-direction, and V is the sample volume.

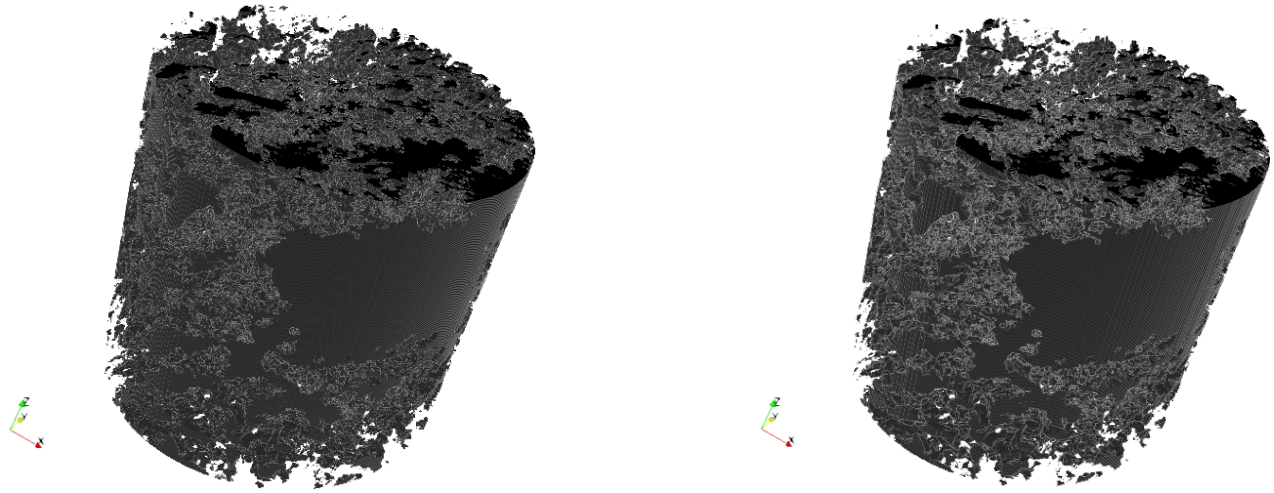

(a) 4.48 μm (b) 8.512 μm

Figure 3: Pore volume of sample 1

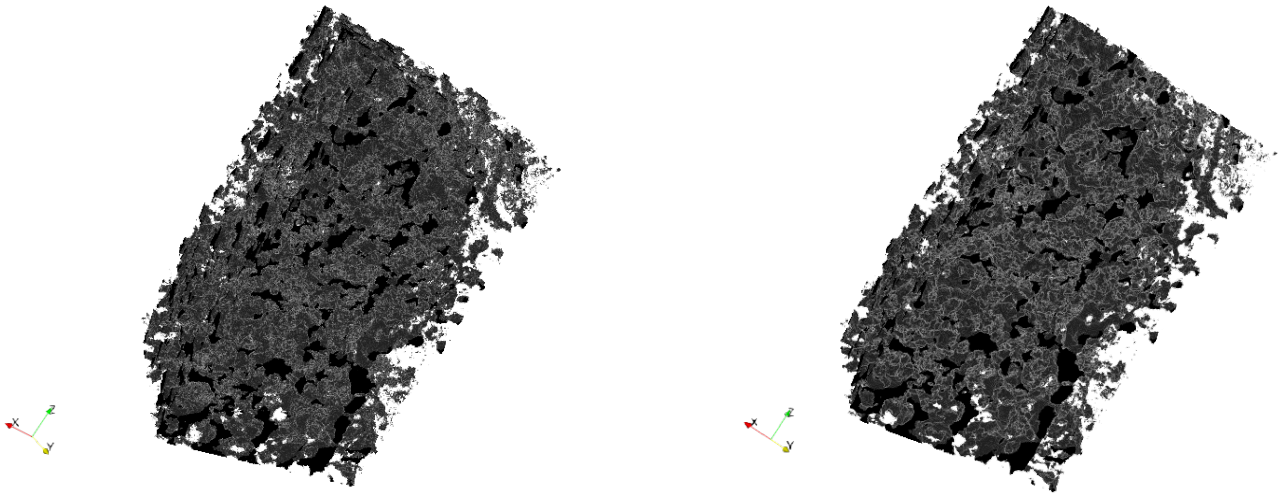

(a) 5.57 μm (b) 11.14 μm

Figure 4: Pore volume of sample 2

2.3 Numerical implementation and Simulation Setup

The Mathematical model composed by Eq. (1 and Eq. (2 is solved using the steady-state solver SimpleFOAM employed to simulate the single phase flow in the porous space. The before mentioned solver is available in OpenFOAM®, a parallel open-source package for the development of numerical solvers for continuum mechanics problems that employs the finite volume method.

The domain is generated based on the X-ray microtomography segmented images, using the blockMesh and the snappyHexMesh utilities provided by OpenFOAM®, considering one cell of the simulation grid as one voxel of the microCT image.

The simulations was performed on a Workstation with 2 processors Intel(R) Xeon(R) Silver 4114 CPU @ 2.20GHz and 256 GB memory RAM. Convergence is considered achieved when residuals go below 10^{-8}. The relaxation factors α_p e α_u are set to 0.9. The fluid flow parameters used for the simulations are listed in Tab 3.

Table 3: Fluid flow parameters.

Pressure (Pa)	Kinematic Viscosity (m^2/s)	Density (kg/m^3)
1	10^{-6}	1000

3. RESULTS

This section presents the results of porosity and permeability obtained after each resample done. The values obtained were compared with those obtained experimentally using Mercury intrusion porosimetry (MIP).

3.1 Estimation of porosity

The segmented images are used to estimate samples porosity. Total porosity is calculated as the ratio between the number of voxels with 0 value present in the image and the total number of voxels, i.e. with values 0 and 1. The results of porosity calculated after each resample are shown in Fig. 5.

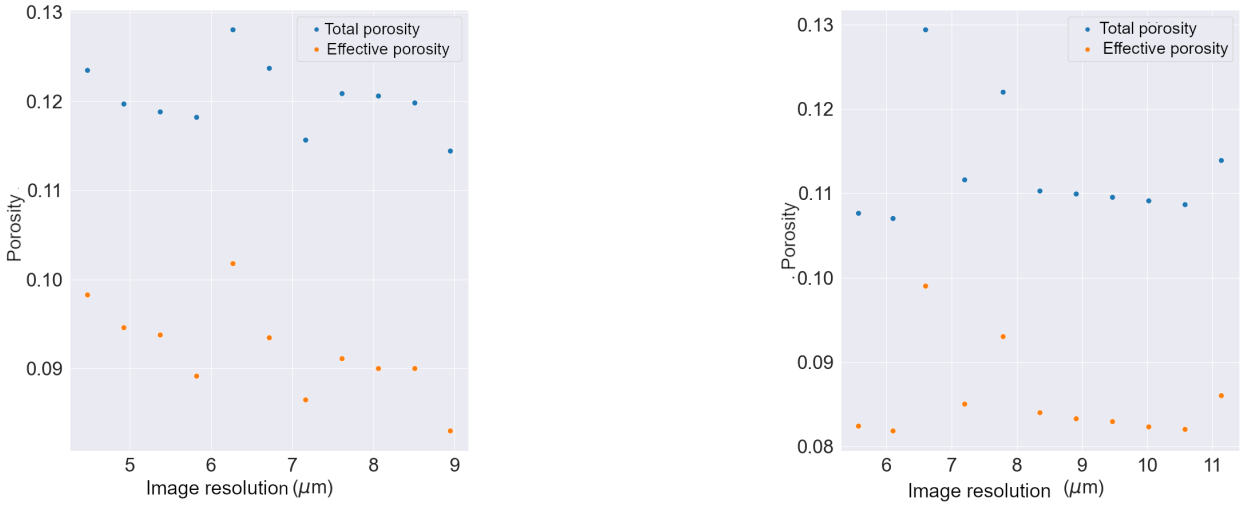

(a) Sample 1

(b) Sample 2

Figure 5: Porosity variation for each sample.

After analysis, we can see that the oscillation in the absolute and effective porosity values is small in relation to the value obtained considering the original resolutions, of 4.48 and 5.57 μm, respectively, at most 0.02 for these two samples.

In relation to the experimental effective porosity values of 0.1384 and 0.1938, for samples 1 and 2 respectively, all porosity values obtained were below, a fact that can be explained by the possible existence of pores below the image resolution that were not considered.

3.2 Estimation of permeability

After the simulations performed on each computational mesh generated from the images that passed through the resample, the permeability results obtained are presents in Fig. 6.

After analysis, we can see that the oscillation in the absolute permeability values is greater than the value obtained considering the original resolutions, of 4.48 and 5.57 μm, respectively. Despite the greater oscillation of the values, they oscillate within the same order of magnitude. This difference in the permeability values can be explained by the decrease in the interconnectivity of the porous system, mainly in the reduction of throats of smaller radius, as can be seen in the Tables 4 and 5 below, that compares the number of pores, pore connections throats and number of throats with radius less than $3\mu m$ in the original resolutions, of 4.48 and $5.57\mu m$, respectively, and after the last resample (8.95 and 11.14 μm).

In addition, we can check in the Figures 7 and 8 with the pore size distribution of samples with original resolution and after the last resizing, that there was a decrease in the range of pore sizes that can to impact the permeability results. The Pore Size Distribution was made in Imago3D, a software that is owned by Laboratório de Meios Porosos e Propriedades Termofísicas (LMPT). In Imago3D, pore size distribution is done by successive opening done in binary 2-D sections, derived from mathematical morphology and using balls with increasing radius (Damiani *et al.*, 2003).

The results presented in the Tables 4 and 5 were generated using commercial software PORE® Project developed by Engineering Simulation and Scientific Software (ESSS). PORE uses pore network modelling technique, which simplifying the porous space using simple geometries to represent the pores and throats.

In relation to the experimental permeability values of $663.57\ mD$ and $372.27\ mD$, for samples 1 and 2 respectively. For Sample 1 the estimated data are larger than the experimental value. This may be due to a narrowing of the pore throats not captured in this image resolution, but captured experimentally. For Sample 2 all permeability values obtained are

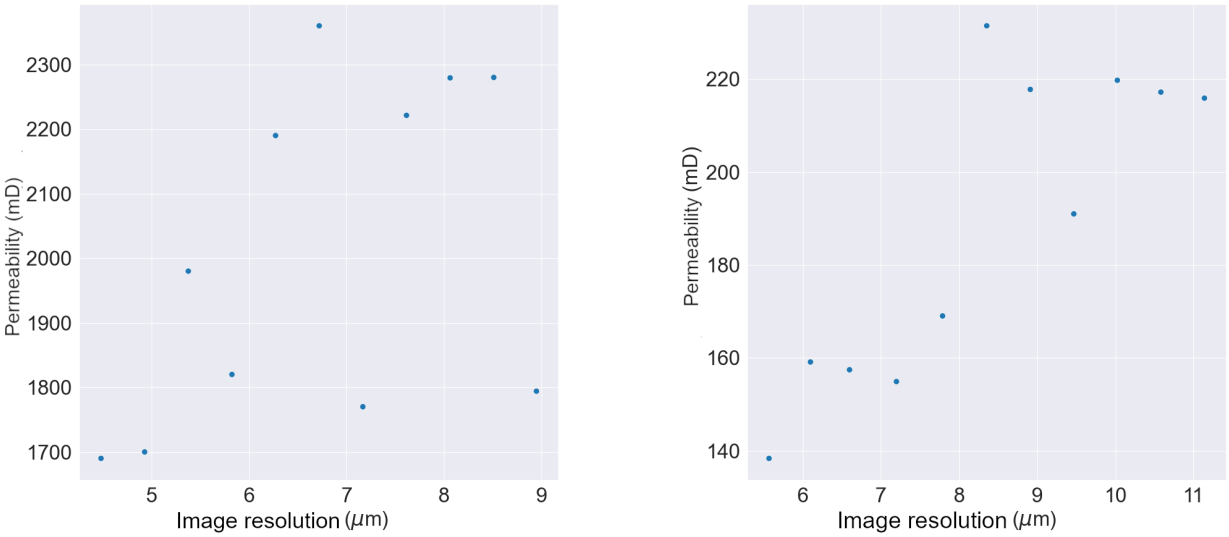

(a) Sample 1 (b) Sample 2

Figure 6: Permeability variation for each sample.

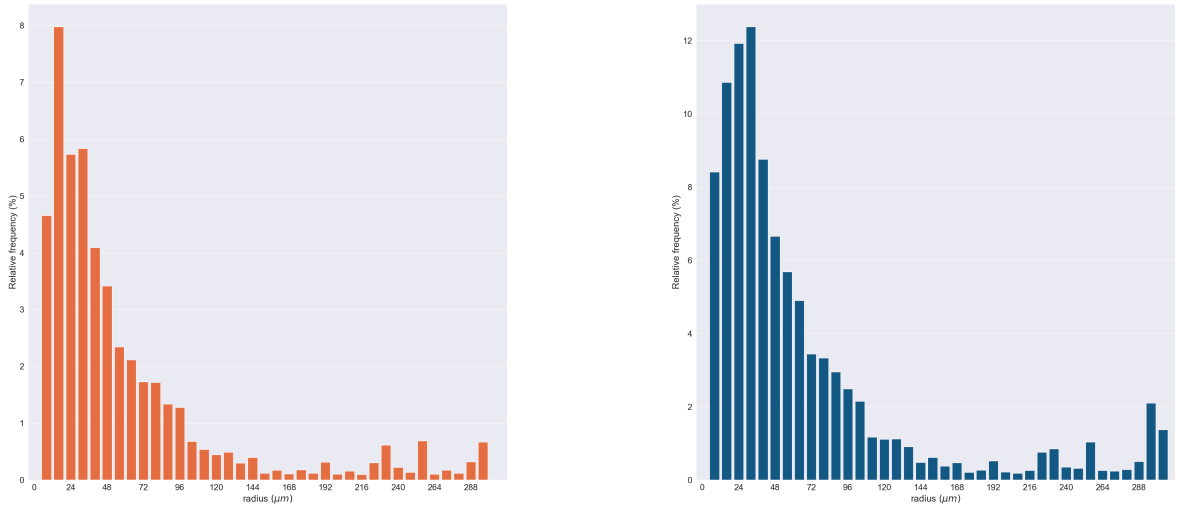

(a) 4.48 μm (b) 8.95 μm

Figure 7: Pore size distribution of sample 1.

Table 4: Comparison between the number of pores and throats before and after resizing.

image resolution (μm)	number of pores	number of throats	number of pores connected	number of throats with radius less than 3 μm
4.48	75942	60188	41269	2851
8.95	32634	24308	15379	365

below but in the same order of magnitude of experimental result.

3.3 Time spent in solver

The solution of the equations is the most expensive part during the whole process from mesh generation to permeability calculation. The times spent during the solver execution are shown in the Tables 6 and 7.

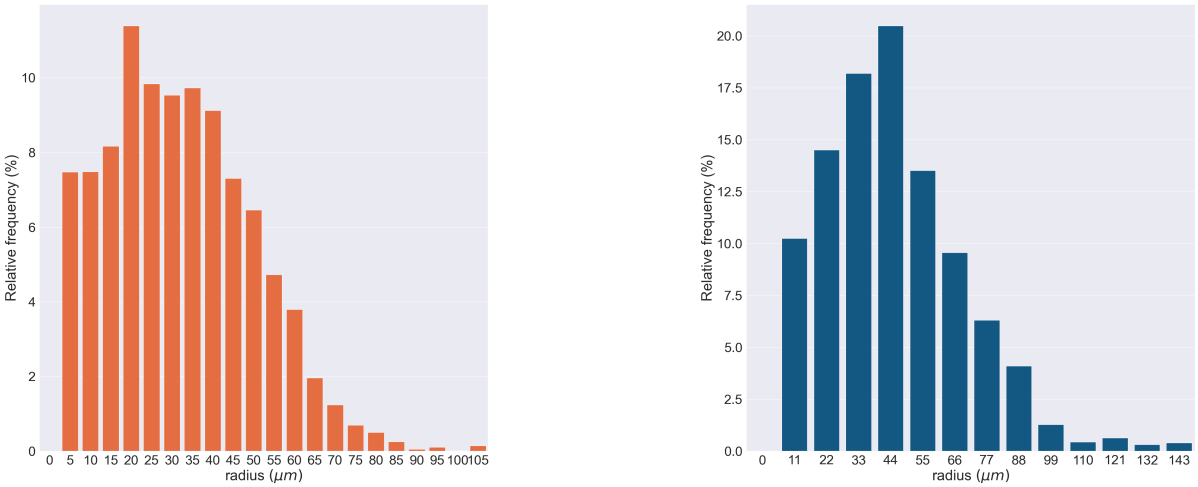

(a) 5.57 μm (b) 11.14 μm

Figure 8: pore size distribution of sample 2.

Table 5: Comparison between the number of pores and throats before and after resizing.

image resolution (μm)	number of pores	number of throats	number of pores connected	number of throats with radius less than 3 μm
5.57	75484	22310	18703	800
11.14	11851	5743	4682	31

Table 6: Time (in hours) spent in the SimpleFOAM solver after Sample 1 resample.

image resolution (μm)	time (h)
4.48	117.84
5.376	14.55
5.824	9.58
6.272	6.92
5.72	5.93
7.168	3.35
7.616	2.76
8.024	2.18
8.512	1.68
8.95	0.90

Table 7: Time (in hours) spent in the SimpleFOAM solver after Sample 2 resample.

image resolution (μm)	time (h)
5.57	1.22
6.1	1.16
6.6	0.99
7.2	0.93
7.79	0.84
8.355	1.39
8.912	1.30
9.469	1.11
10.026	1.18
10.583	0.35
11.14	0.55

The computational time, after resizing, had a drop of 97.635% for sample 1 and 45.26% for sample 2.

4. CONCLUSIONS

In this work we study the impact of the microCT image resizing on estimated porosity and permeability values. The microCT images used were obtained from two different carbonate core-plug subsamples of the Jandaíra Formation, that was subjected to the karstification process. The Stokes equations are employed to numerically simulate this fluid flow, and from velocity fields, permeability estimates can be obtained. The results show that the porosity results suffered little change after each resizing. The permeability results showed a great variation in relation to initial permeability values, i.e., calculated on the images with the original resolutions, but remains in the same order of magnitude. Regarding the experimental values, both the porosity values and the permeability values are different, but remains in the same order of magnitude, with the exception of the permeability values obtained from Sample 1, whose values are higher because it may have a funneling of the pore throats in pores at lower resolutions. It was also shown that the reduction in computational times spent in SimpleFOAM was reduced to about 97.6% and 45.3%, for an increase of 2 times the original resolution. Therefore, for the two samples studied, we can conclude that the resizing using the Lanczos method did not significantly affect the porosity, but affecting the permeability. However, for the two pore systems analyzed, the significant computational cost reduction and the maintenance of the permeability value in the same order of magnitude, enables the use of the resized image.

5. ACKNOWLEDGEMENTS

This work has been supported by the following Brazilian research agency CNPQ. The authors thank ESSS for the license of the PORE software used in this work.

6. REFERENCES

Al-Ansi, N., Gharbi, O., Raeini, A.Q., Yang, J., Iglauer, S. and Blunt, M.J., 2013. "Influence of micro-computed tomography image resolution on the predictions of petrophysical properties". In *IPTC 2013: International Petroleum Technology Conference*. European Association of Geoscientists & Engineers, pp. cp–350.

Al-Marzouqi, H., 2018. "Digital rock physics: Using ct scans to compute rock properties". *IEEE Signal Processing Magazine*, Vol. 35, No. 2, pp. 121–131. doi:10.1109/MSP.2017.2784459.

Alyafei, N., Raeini, A.Q., Paluszny, A. and Blunt, M.J., 2015. "A sensitivity study of the effect of image resolution on predicted petrophysical properties". *Transport in Porous Media*, Vol. 110, No. 1, pp. 157–169.

Arns, C.H., Bauget, F., Limaye, A., Sakellariou, A., Senden, T., Sheppard, A., Sok, R.M., Pinczewski, V., Bakke, S., Berge, L.I. *et al.*, 2005. "Pore scale characterization of carbonates using x-ray microtomography". *Spe Journal*, Vol. 10, No. 04, pp. 475–484.

Bohnsack, D., Potten, M., Pfrang, D., Wolpert, P. and Zosseder, K., 2020. "Porosity–permeability relationship derived from upper jurassic carbonate rock cores to assess the regional hydraulic matrix properties of the malm reservoir in the south german molasse basin". *Geothermal Energy*, Vol. 8, No. 1, pp. 1–47.

Buades, A., Coll, B. and Morel, J.M., 2005. "A non-local algorithm for image denoising". In *2005 IEEE Computer Society Conference on Computer Vision and Pattern Recognition (CVPR'05)*. IEEE, Vol. 2, pp. 60–65.

Damiani, M., Fern, C., Bueno, A. and Dos Santos, L., 2003. "Characterization of reservoir rocks from image analysis on imago software". p. 4.

Distante, A. and Distante, C., 2020. *Handbook of Image Processing and Computer Vision: Volume 2: From Image to Pattern*. Springer International Publishing. ISBN 9783030423742. URL `https://books.google.com.br/books?id=hCroDwAAQBAJ`.

FEI, 2014. "Avizo 8 software".

Han, C. and Baek, J., 2019. *Opt. Express*, Vol. 27, No. 7, pp. 10108–10126. doi:10.1364/OE.27.010108. URL `http://opg.optica.org/oe/abstract.cfm?URI=oe-27-7-10108`.

Latief, F., Fauzi, U., Irayani, Z. and Dougherty, G., 2017. "The effect of x-ray micro computed tomography image resolution on flow properties of porous rocks". *Journal of microscopy*, Vol. 266, No. 1, pp. 69–88.

Mostaghimi, P., Blunt, M.J. and Bijeljic, B., 2013. "Computations of absolute permeability on micro-ct images". *Mathematical Geosciences*, Vol. 45, No. 1, pp. 103–125.

Peng, S., Hu, Q., Dultz, S. and Zhang, M., 2012. "Using x-ray computed tomography in pore structure characterization for a berea sandstone: Resolution effect". *Journal of hydrology*, Vol. 472, pp. 254–261.

Semmler, W. and Schwaiger, M., 2008. *Molecular Imaging I*. Handbook of Experimental Pharmacology. Springer Berlin Heidelberg. ISBN 9783540727170.

Sheppard, A.P., Sok, R.M. and Averdunk, H., 2004. "Techniques for image enhancement and segmentation of tomographic images of porous materials". *Physica A: Statistical mechanics and its applications*, Vol. 339, No. 1-2, pp. 145–151.

Soulaine, C., Gjetvaj, F., Garing, C., Roman, S., Russian, A., Gouze, P. and Tchelepi, H.A., 2016. "The impact of sub-resolution porosity of x-ray microtomography images on the permeability". *Transport in porous media*, Vol. 113, No. 1, pp. 227–243.

Weinert, S., Bär, K. and Sass, I., 2021. "Database of petrophysical properties of the mid-german crystalline rise". *Earth System Science Data*, Vol. 13, No. 3, pp. 1441–1459. doi:10.5194/essd-13-1441-2021. URL `https://essd.copernicus.org/articles/13/1441/2021/`.

7. RESPONSIBILITY NOTICE

The following text, properly adapted to the number of authors, must be included in the last section of the paper: The author(s) is (are) solely responsible for the printed material included in this paper.